

Bounds on the rise of total cross section from LHC7 and LHC8 data

D. A. Fagundes^a, M. J. Menon^b, P. V. R. G. Silva^b

^a*Departamento de Ciências Exatas e Educação, Universidade Federal de Santa Catarina - Campus Blumenau, 89065-300 Blumenau, SC, Brazil*

^b*Instituto de Física Gleb Wataghin, Universidade Estadual de Campinas - UNICAMP 13083-859 Campinas, SP, Brazil*

Abstract

Recent measurements of the proton-proton total cross section σ_{tot} at 7 and 8 TeV by the TOTEM and ATLAS Collaborations are characterized by some discrepant values: the TOTEM data suggest a rise of the cross section with the energy faster than the ATLAS data. Attempting to quantify these different behaviors, we develop new analytical fits to σ_{tot} and ρ data from pp and $\bar{p}p$ scattering in the energy region 5 GeV - 8 TeV. The dataset comprises all the accelerator data below 7 TeV and we consider three ensembles by adding: either only the TOTEM data (T), or only the ATLAS data (A), or both sets (T+A). For the purposes, we use our previous RRPL γ parametrization for $\sigma_{tot}(s)$, consisting of two Reggeons (RR), one critical Pomeron (P) and a leading log-raised-to-gamma (L γ) contribution (with γ as a free fit parameter), *analytically* connected to $\rho(s)$ through singly-subtracted derivative dispersion relations and energy scale fixed at the physical threshold. The data reductions with ensembles T and A present good agreement with the experimental data analyzed and cannot be distinguished on statistical grounds. The quality of the fit is not as good with ensemble T+A. The fit results provide $\gamma \sim 2.3 \pm 0.1$ (T), 2.0 ± 0.1 (A), 2.2 ± 0.2 (T+A), with $\chi^2/\text{DOF} \sim 1.07$ (T), 1.09 (A), 1.14 (T+A), suggesting extrema bounds for γ given by 1.9 and 2.4. Fits with $\gamma = 2$ (fixed) are also developed and discussed.

Keywords: Hadron-induced high- and super-high-energy interactions, Total cross-sections, Asymptotic problems and properties 13.85.-t, 13.85.Lg, 11.10.Jj

Published in Nuclear Physics A (2017)

Contents

1. Introduction
2. Analytical Parametrization
3. Ensembles, Fits Procedures and Fit Results
 - 3.1 Experimental Data and Ensembles
 - 3.2 Fit Procedures
 - 3.3 Fit Results
4. Summary, Conclusions and Final Remarks
- Appendix A. Comments on the Dataset and Fit Procedures

1. Introduction

The elastic scattering of hadrons at high energies is characterized by its amplitude A as a function of the c.m. energy and transferred momentum squared in the collision process, s and t . These soft scattering states constitute one of the great challenges for the QCD, because, as a long distance phenomena, its investigation demands a nonperturbative approach and presently, a formal approach from first principles, able to provide $A = A(s, t)$, is still absent.

In the forward scattering, the elastic amplitude is connected with two important physical observables: the total cross section (optical theorem),

$$\sigma_{tot}(s) = \frac{\text{Im } A(s, t = 0)}{s} \quad (1)$$

and the ρ parameter (related to the phase of the amplitude),

$$\rho(s) = \frac{\text{Re } A(s, t = 0)}{\text{Im } A(s, t = 0)}. \quad (2)$$

A fundamental formal result on the rise of $\sigma_{tot}(s)$, at asymptotic energies ($s \rightarrow \infty$), is the upper bound by Froissart, Lukaszuk, Martin [1–4]

$$\sigma_{tot}(s) < c \ln^2(s/s_0), \quad (3)$$

where s_0 is an unspecified energy scale and the pre-factor on the right-hand side is bounded by π/m_π^2 , where m_π is the pion mass [4].

Beyond specific phenomenological models, an important approach in the investigation of $\sigma_{tot}(s)$ and $\rho(s)$ is the forward amplitude analysis, characterized by Regge-Gribov analytical parametrization for $\sigma_{tot}(s)$, connected with $\rho(s)$ by means of dispersion relations or asymptotic uniqueness and analytical or numerical methods (for example, [5–14]).

A typical behavior emerging from several analyses favors a leading $\ln^2 s$ dependence for $\sigma_{tot}(s)$ at the highest energies [8, 9, 11–14]. In a nonperturbative QCD approach this behavior has been also recently predicted under specific conditions [15, 16].

Some authors have considered a leading $\ln^\gamma s$ dependence, with γ as a free fit parameter. Different approaches using different datasets indicated $\gamma = 2.10 \pm 0.10$ [5] (1977), $2.24_{-0.31}^{+0.35}$ [6] (1993) and in our more recent analyses, $\gamma = 2.2 - 2.4$ [17–20], with the last updated result $\gamma = 2.23 \pm 0.11$ [20] (2013). In the theoretical context, the possibility of a rise of $\sigma_{tot}(s)$ faster than $\ln^2 s$, without violating unitarity, is discussed in [21]. It should be also noted that Eqs. (3-4) are intended for $s \rightarrow \infty$ and presently, experimental data from accelerators have been obtained up to $\sqrt{s} = 8$ TeV. To a certain extent contrasting with the above γ values, the COMPAS group (PDG) has quoted the value 1.98 ± 0.01 [13, 14].

In the experimental context, the recent data from LHC7 and LHC8 are expected to provide fundamental information for amplitude analyses. These new experimental information comprise 5 measurements of σ_{tot} at 7 TeV (4 data obtained by the TOTEM Collaboration [22–24] and 1 datum by the ATLAS Collaboration [25]), 6 measurements at 8 TeV (5 data by TOTEM [26–28] and 1 datum by ATLAS [29]) and one measurement of ρ at 8 TeV by the TOTEM Collaboration [28]. All these total cross section data are displayed in Table 1,

Table 1: Measurements of the pp total cross section from LHC7 and LHC8: central value (σ_{tot}), statistical uncertainties ($\Delta\sigma_{tot}^{stat.}$), systematic uncertainties ($\Delta\sigma_{tot}^{syst.}$), total uncertainty from quadrature ($\Delta\sigma_{tot}$).

\sqrt{s} (TeV)	σ_{tot} (mb)	$\Delta\sigma_{tot}^{stat.}$ (mb)	$\Delta\sigma_{tot}^{syst.}$ (mb)	$\Delta\sigma_{tot}$ (mb)	Collaboration [reference]
7.0	98.3	0.2	2.8	2.8	TOTEM [22]
	98.6	-	2.2	2.2	TOTEM [23]
	98.0	-	2.5	2.5	TOTEM [24]
	99.1	-	4.3	4.3	TOTEM [24]
	95.35	0.38	1.304	1.36	ATLAS [25]
8.0	101.7	-	2.9	2.9	TOTEM [26]
	101.5	-	2.1	2.1	TOTEM [27]
	101.9	-	2.1	2.1	TOTEM [27]
	102.9	-	2.3	2.3	TOTEM [28]
	103.0	-	2.3	2.3	TOTEM [28]
	96.07	0.18	0.85 ± 0.31	0.92	ATLAS [29]

where we have expressed as systematic also the uncertainties associated with extrapolations and error propagated from uncertainties in the fit parameters.

However, TOTEM and ATLAS data present discrepant values. In special, at 8 TeV the ATLAS datum [29] and the latest measurement by the TOTEM Collaboration [28] differ by

$$\frac{\sigma_{tot}^{\text{TOTEM}} - \sigma_{tot}^{\text{ATLAS}}}{\Delta\sigma_{tot}^{\text{TOTEM}}} = \frac{103 - 96.07}{2.3} = 3.0.$$

This ratio results 7.5 if the ATLAS uncertainty is considered.

In this situation, it may be important and instructive to attempt to quantify these discrepancies through an amplitude analysis, able to test statistical consistency with experimental data at lower energies, as well as estimating uncertainty regions for extrapolations to higher (and asymptotic) energies. In this sense, the log-raised-to-gamma leading term provides a useful tool through the γ values (and the pre-factor values) that can be determined from different fits to different datasets¹. Moreover, the extracted γ values provide also information on the proximity and/or consistency with the particular case $\gamma = 2$ (Froissart, Lukaszuk, Martin bound).

To this end, we develop here new fits with our RRPL γ parametrization for $\sigma_{tot}(s)$, analytically connected to $\rho(s)$ through singly-subtracted derivative dispersion relations [17–20]. We consider either γ as a free fit parameter or $\gamma = 2$ (fixed). The dataset comprises all the accelerator data from pp and $\bar{p}p$ elastic scattering above 5 GeV and up to 8 TeV. For σ_{tot} , including the data below 7 TeV, we consider three ensembles by adding: either only the TOTEM data (ensemble T), or only the ATLAS data (ensemble A), or both sets (ensemble T+A).

¹Another useful parameter is the soft Pomeron intercept, related to the simple pole leading contribution, s^ϵ , as done in [10] in case of $\bar{p}p$ scattering at 1.8 TeV and cosmic-ray estimations for σ_{tot} .

Our main conclusions are the following: (1) the data reductions with ensembles T or A present good agreement with the experimental data analyzed and cannot be distinguished on statistical grounds; (2) the quality of the fit is not as good in case of ensemble T+A and the curves lies between the TOTEM and ATLAS data; (3) the fits with γ free or fixed to 2 are also indistinguishable on statistical grounds; (4) we infer upper and lower bounds for γ given by 2.4 and 1.9.

The article is organized as follows. In Section 2 present our analytical parametrization. In Section 3 we refer to the experimental data analyzed (defining the three ensembles) and present the fits procedures and results. Our conclusions and final remarks are the contents of Section 4.

2. Analytical Parametrization

This analytical model has been introduced in [17] and further developed, extended and discussed in [18–20]. It consists of two assumptions related to $\sigma_{tot}(s)$ and $\rho(s)$.

The total cross section is given by the parametrization introduced by Amaldi et al. in the 1970s [5]:

$$\sigma_{tot}(s) = a_1 \left[\frac{s}{s_0} \right]^{-b_1} + \tau a_2 \left[\frac{s}{s_0} \right]^{-b_2} + \alpha + \beta \ln^\gamma \left(\frac{s}{s_0} \right), \quad (4)$$

where $\tau = -1$ (+1) for pp ($\bar{p}p$) scattering and $a_1, b_1, a_2, b_2, \alpha, \beta, \gamma$ are real free fit parameters. Here, the energy scale is fixed at the physical threshold (see [20] for discussions on this choice):

$$s_0 = 4m_p^2 \sim 3.521 \text{ GeV}^2.$$

The $\rho(s)$ dependence is analytically determined through singly subtracted derivative dispersion relations, using the Kang and Nicolescu representation [30] and reads:

$$\rho(s) = \frac{1}{\sigma_{tot}(s)} \left\{ \frac{K_{eff}}{s} + T_R(s) + T_P(s) \right\}, \quad (5)$$

where K_{eff} is an *effective subtraction constant* (discussed below) and the terms (T) associated with Reggeon (R) and Pomeron (P) contributions are given by

$$T_R(s) = -a_1 \tan \left(\frac{\pi b_1}{2} \right) \left[\frac{s}{s_0} \right]^{-b_1} + \tau a_2 \cot \left(\frac{\pi b_2}{2} \right) \left[\frac{s}{s_0} \right]^{-b_2}, \quad (6)$$

$$T_P(s) = \mathcal{A} \ln^{\gamma-1} \left(\frac{s}{s_0} \right) + \mathcal{B} \ln^{\gamma-3} \left(\frac{s}{s_0} \right) + \mathcal{C} \ln^{\gamma-5} \left(\frac{s}{s_0} \right), \quad (7)$$

where

$$\begin{aligned} \mathcal{A} &= \frac{\pi}{2} \beta \gamma, & \mathcal{B} &= \frac{1}{3} \left[\frac{\pi}{2} \right]^3 \beta \gamma [\gamma - 1][\gamma - 2], \\ \mathcal{C} &= \frac{2}{15} \left[\frac{\pi}{2} \right]^5 \beta \gamma [\gamma - 1][\gamma - 2][\gamma - 3][\gamma - 4]. \end{aligned} \quad (8)$$

We refer to the subtraction constant as *effective* because, as a free fit parameter, it takes account of the constant (not zero) lower limit in the Integral Dispersion Relation, which is replaced by the derivative form. In a *high-energy approximation* this lower limit, given by the energy threshold $s_0 = 4m_p^2$, is assumed as zero. However, once taken into account, it results in a series expansion whose first order term ($1/s$) can be absorbed in the K/s term in the dispersion relation, defining our *effective subtraction constant*. As a consequence, its introduction means that, in first order, the high-energy approximation is not included, which gives support for fits at intermediated and low energies (above the energy cutoff, $\sqrt{s_{min}} = 5$ GeV). These aspects related to the role and practical applicability of the subtraction constant as a free fit parameter are discussed in [18], Section 2.3.2, [20], Section A.2 and [31], Section 4.4.

In the particular case of $\gamma = 2$, from Eq. (8), $\mathcal{A} = \pi\beta$, $\mathcal{B} = \mathcal{C} = 0$ and from Eqs. (4-7), the expressions for $\sigma_{tot}(s)$ and $\rho(s)$ have the *same analytical structure* as those selected by the COMPETE Collaboration [8, 9] and used in the successive editions by the PDG [13, 14], except for the presence here of the effective subtraction constant and the fixed energy scale (not associated with a free parameter). Also, our pre-factor β is not related to the energy scale.

Inspired by the COMPETE notation [8] we can express these two cases as RRPL γ and RRPL2 models. Given the same sub-leading terms, for short, we shall refer to them only as L γ and L2 models.

3. Ensembles, Fits Procedures and Fit Results

3.1. Experimental Data and Ensembles

Our dataset on σ_{tot} and ρ comprises all the accelerator data from pp and $\bar{p}p$ elastic scattering above 5 GeV [32] (same cutoff used in the COMPETE and PDG analyses), including all published results from LHC7 and LHC8 by the TOTEM and ATLAS Collaborations (Table 1). The recent measurement of ρ at 8 TeV by the TOTEM Collaboration [28] is also included in the dataset. Although not taking part in the data reductions, we will display in the figures, as illustration, some estimations of σ_{tot} from cosmic-ray experiments: ARGO-YBJ results at 100 - 400 GeV [33], Auger result at 57 TeV [34] and Telescope Array (TA) result at 95 TeV [35].

We consider three ensembles for σ_{tot} , all of them including the data below 7 TeV and distinguished by adding: only the TOTEM data (ensemble T), or only the ATLAS data (ensemble A), or both datasets (ensemble T+A).

3.2. Fit Procedures

The nonlinearity of the fit demands the choice of initial values for the free parameters and that is an important point. As in our previous analyses, we develop data reductions with both the L2 and L γ models defined in Section 2: first with L2 and then with L γ (by letting free the parameter γ) and using as initial values for this last fit the results of the former. For L2 we use as initial values for the free parameters the last result by the COMPAS group

from PDG 2016 [14]:

$$\begin{aligned} a_1 &= 13.07 \text{ mb}, & b_1 &= 0.4473, & a_2 &= 7.394 \text{ mb}, & b_2 &= 0.5486, \\ \alpha &= 34.41 \text{ mb}, & \beta &= 0.272 \text{ mb}. \end{aligned}$$

Since the subtraction constant is absent in the COMPAS parametrization we consider the initial value 0 for K_{eff} .

The above procedure for feedbacks (PDG 2016 \rightarrow L2 \rightarrow L γ) is applied to each one of the three ensembles.

As in our previous analysis, the data reductions have been performed with the objects of the class TMinuit of ROOT Framework [36]. We have employed the default MINUIT error analysis [37] with the *selective criteria* explained in [19] (section 2.2.4). Variances and covariances associated with each free parameter are used in the analytic evaluation of the uncertainty regions associated with the fitted and predicted quantities. As tests of goodness-of-fit we shall consider the chi-square per degree of freedom (χ^2/ν) and the corresponding integrated probability, $P(\chi^2)$ [38].

3.3. Fit Results

The fit results and statistical information on the goodness-of-fit with models L2 and L γ to ensembles T, A and T+A are displayed in Table 2. For each ensemble, the corresponding curves (with the uncertainty regions from error propagation) and the experimental data are shown in Figure 1 from model L2 and in Figure 2 from model L γ .

For each fit result (models L2, L γ and ensembles T, A, T+A), the predictions for σ_{tot} and ρ at some energies of interest in pp scattering are displayed in Tables 3 (L2 model) and 4 (L γ model).

In this analysis all the TOTEM data have been considered as independent in the data reductions, including the two points from [27] and the two points from [28] (Table 1). See Appendix A for a discussion on this respect.

Table 2: Fit results with models L2 and L γ to ensembles T, A and T+A. Parameters a_1, a_2, α, β in mb, K_{eff} in mbGeV² and b_1, b_2, γ dimensionless. Energy scale fixed, $s_0 = 4m_p^2 = 3.521 \text{ GeV}^2$.

Ensemble:	TOTEM		ATLAS		TOTEM + ATLAS	
Model:	L2	L γ	L2	L γ	L2	L γ
a_1	32.11(60)	31.5(1.3)	32.39(86)	32.4(1.0)	32.16(67)	31.60(98)
b_1	0.381(17)	0.528(57)	0.435(19)	0.438(57)	0.406(16)	0.484(84)
a_2	16.98(72)	17.10(74)	17.04(72)	17.04(72)	17.01(72)	17.07(73)
b_2	0.545(13)	0.546(13)	0.545(13)	0.545(13)	0.545(13)	0.546(13)
α	29.25(44)	34.0(1.1)	30.88(35)	31.0(2.1)	30.06(34)	32.8(2.2)
β	0.2546(39)	0.103(29)	0.2347(35)	0.231(83)	0.2451(28)	0.151(71)
γ	2 (fixed)	2.301(98)	2 (fixed)	2.01(12)	2 (fixed)	2.16(16)
K_{eff}	50(17)	109(36)	74(20)	75(27)	61(17)	90(42)
ν	242	241	235	234	244	243
χ^2/ν	1.09	1.07	1.08	1.09	1.15	1.14
$P(\chi^2)$	0.150	0.213	0.177	0.166	0.059	0.063

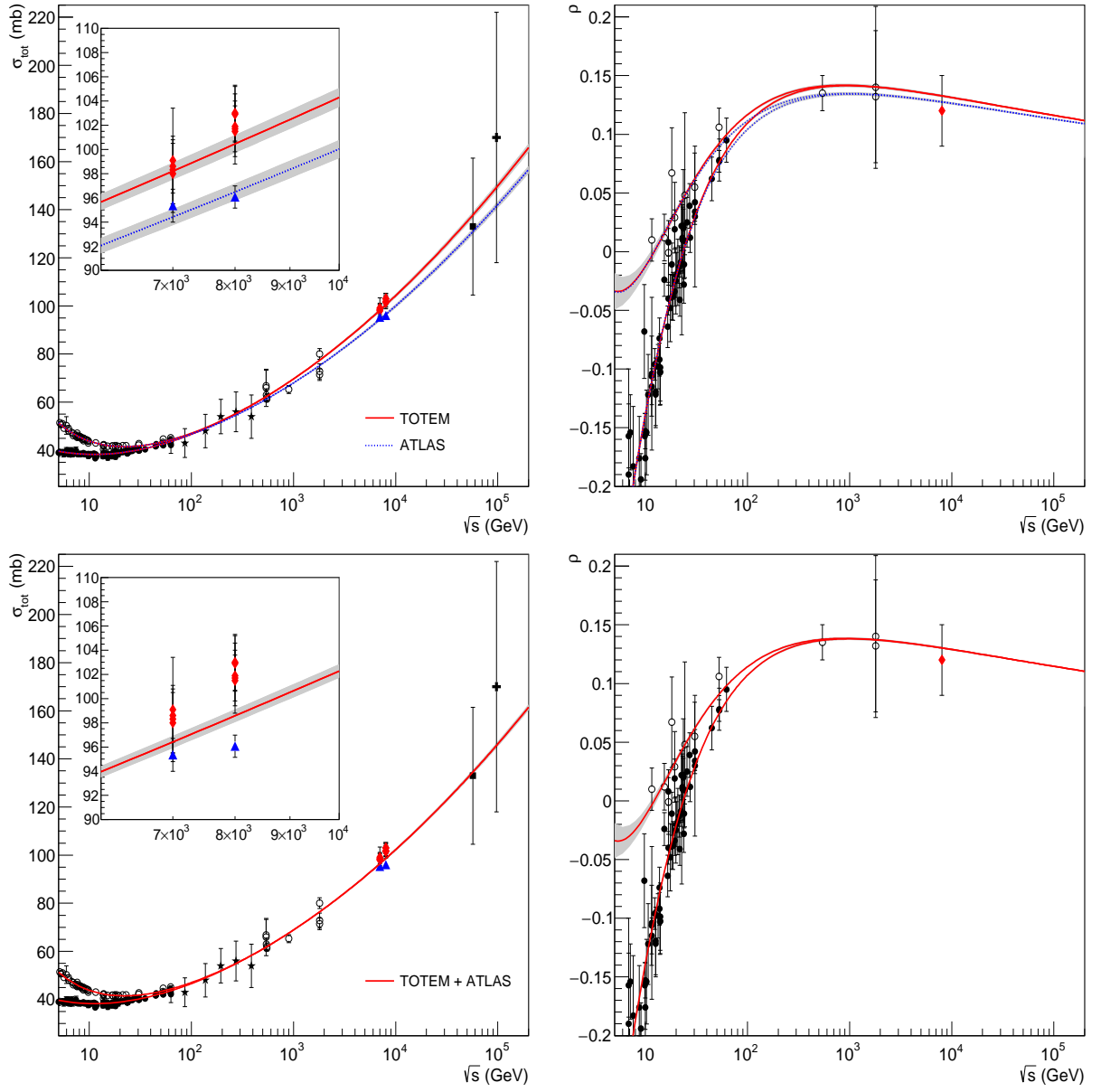


Figure 1: Data reductions to σ_{tot} (left) and ρ (right) from pp (black circles) and $\bar{p}p$ (white circles) scattering. Fit results with the **L2 model** to ensembles T and A (above) and T+A (below).

Table 3: Predictions for σ_{tot} and ρ with the L2 model.

\sqrt{s} (TeV)	TOTEM		ATLAS		TOTEM + ATLAS	
	σ_{tot} (mb)	ρ	σ_{tot} (mb)	ρ	σ_{tot} (mb)	ρ
13	108.94(86)	0.1296(10)	104.31(81)	0.12489(92)	106.76(61)	0.12740(75)
14	110.28(88)	0.12915(96)	105.55(83)	0.12447(91)	108.04(63)	0.12694(74)
57	137.8(1.3)	0.11980(73)	130.9(1.2)	0.11625(69)	134.51(92)	0.11813(57)
95	148.8(1.5)	0.11646(66)	141.0(1.4)	0.11324(63)	145.1(1.0)	0.11494(52)

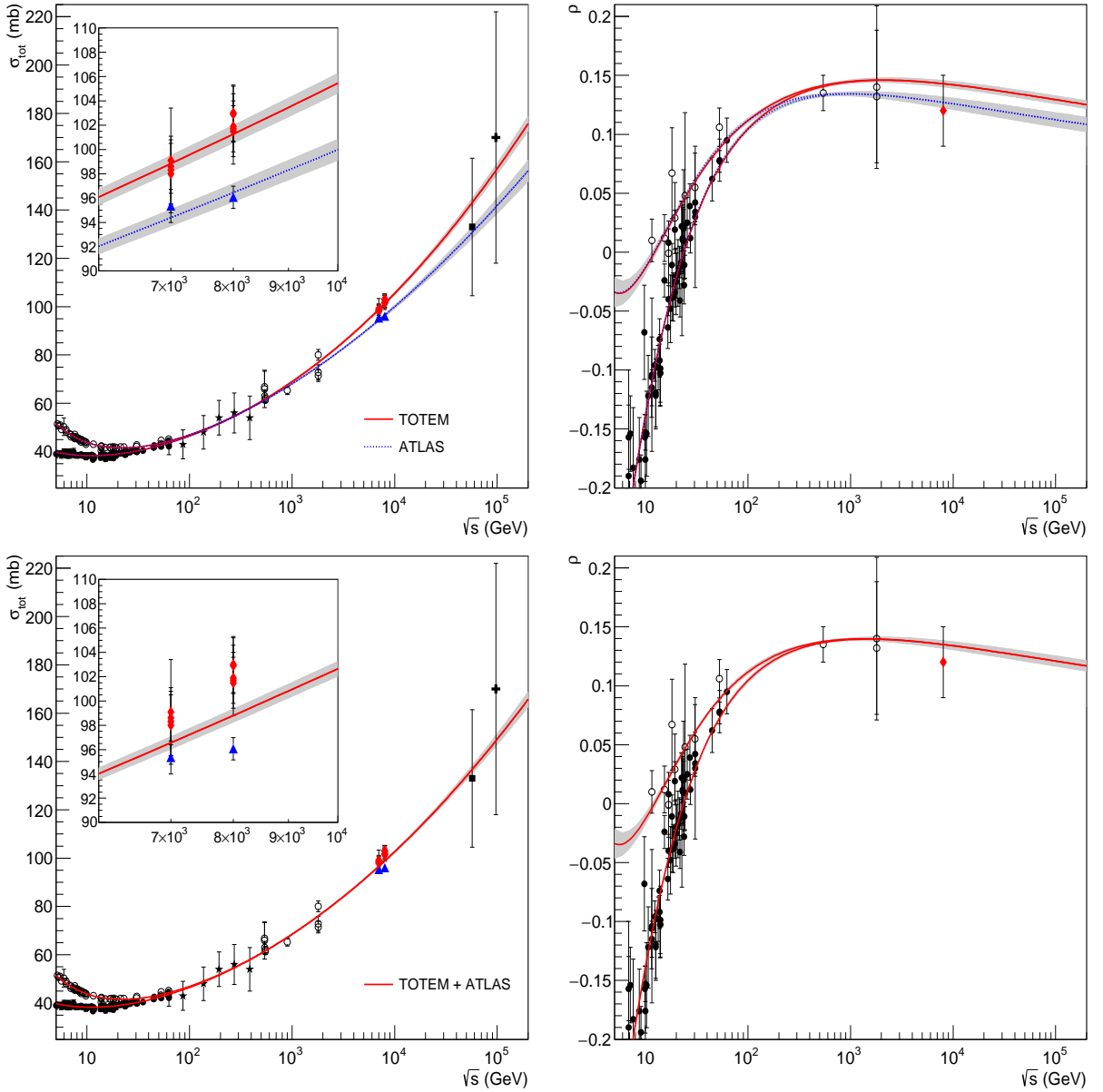


Figure 2: Data reductions to σ_{tot} (left) and ρ (right) from pp (black circles) and $\bar{p}p$ (white circles) scattering. Fit results with the $L\gamma$ model to ensembles T and A (above) and T+A (below).

Table 4: Predictions for σ_{tot} and ρ with the $L\gamma$ model.

\sqrt{s} (TeV)	TOTEM		ATLAS		TOTEM + ATLAS	
	σ_{tot} (mb)	ρ	σ_{tot} (mb)	ρ	σ_{tot} (mb)	ρ
13	110.7(1.2)	0.1417(47)	104.34(97)	0.1251(44)	107.39(94)	0.1333(63)
14	112.1(1.3)	0.1413(47)	105.6(1.0)	0.1247(44)	108.8(1.0)	0.1329(64)
57	143.4(2.8)	0.1337(52)	131.0(2.2)	0.1165(51)	137.0(2.8)	0.1251(73)
95	156.2(3.6)	0.1306(52)	141.2(2.8)	0.1135(52)	148.4(3.7)	0.1221(75)

4. Summary, Conclusions and Final Remarks

Attempting to quantify and investigate the consequences of discrepant measurements of the total cross section by the TOTEM and ATLAS Collaborations, we have developed 6 fits to σ_{tot} and ρ data from pp and $\bar{p}p$ scattering in the energy region 5 GeV - 8 TeV. We applied the L2 and $L\gamma$ models (Section 2) to three ensembles: T, A and T+A (Section 3). The fit results are presented in Table 2 and Figures 1 and 2. In what follows we first refer to the results obtained with ensembles A and T and after that to those obtained with ensemble T+A.

Ensembles T and A indicate different scenarios for the rise of $\sigma_{tot}(s)$, as shown in Figures 1 and 2. These different behaviors can be quantified by two parameters associated with model $L\gamma$ (Table 2): $\beta \sim 0.10 \pm 0.03$ mb, $\gamma \sim 2.3 \pm 0.1$ (T) and $\beta \sim 0.23 \pm 0.08$ mb, $\gamma \sim 2.0 \pm 0.1$ (A). From these results we can infer as extrema bounds for γ the values 1.9 and 2.4. However, with ensembles T or A and models L2 or $L\gamma$, the fits provide $\chi^2/\nu \sim 1.1$ and therefore the results can not be distinguished on statistical grounds.

Let us focus now on the experimental data presently available, namely ensemble T+A. The fit results with models L2 and $L\gamma$ are equivalent on statistical grounds: $\chi^2/\nu = 1.15$ (L2) and 1.14 ($L\gamma$), or $P(\chi^2) \sim 0.06$ in both cases. From Figures 1 and 2 (L2 and $L\gamma$), the curves within the uncertainty regions lie essentially between the TOTEM and ATLAS data. At 8 TeV, they reach the lower end of the TOTEM uncertainties and lie above the ATLAS datum, namely this point is not described by both models. For example, the results within this ensemble for σ_{tot} at 8 TeV are 98.58 ± 0.52 mb (L2) and 98.83 ± 0.60 mb ($L\gamma$) and the differences between these predictions and the ATLAS datum,

$$\frac{\sigma_{tot}^{\text{Predicted}} - \sigma_{tot}^{\text{ATLAS}}}{\Delta\sigma_{tot}^{\text{ATLAS}}},$$

read 2.7 (L2) and 3.0 ($L\gamma$). With model L2 we obtained $\beta = 0.2451 \pm 0.028$ mb, which is below the latest PDG value, $\beta_{\text{PDG}} = 0.2720 \pm 0.048$ mb [14]. With model $L\gamma$, $\beta = 0.151 \pm 0.071$ mb and $\gamma = 2.16 \pm 0.16$. It is interesting to note that this γ -value is in agreement with the result obtained by Amaldi et al., forty years ago (data up to 62.5 GeV), namely $\gamma_{\text{A}} = 2.10 \pm 0.10$ [5].

Within each one of the three ensembles, all the predictions for σ_{tot} at 13 TeV with models L2 and $L\gamma$ (Tables 3 and 4) are in agreement within the uncertainties and cannot be distinguished. However, the results from distinct ensembles present differences, as illustrated in Figure 3.

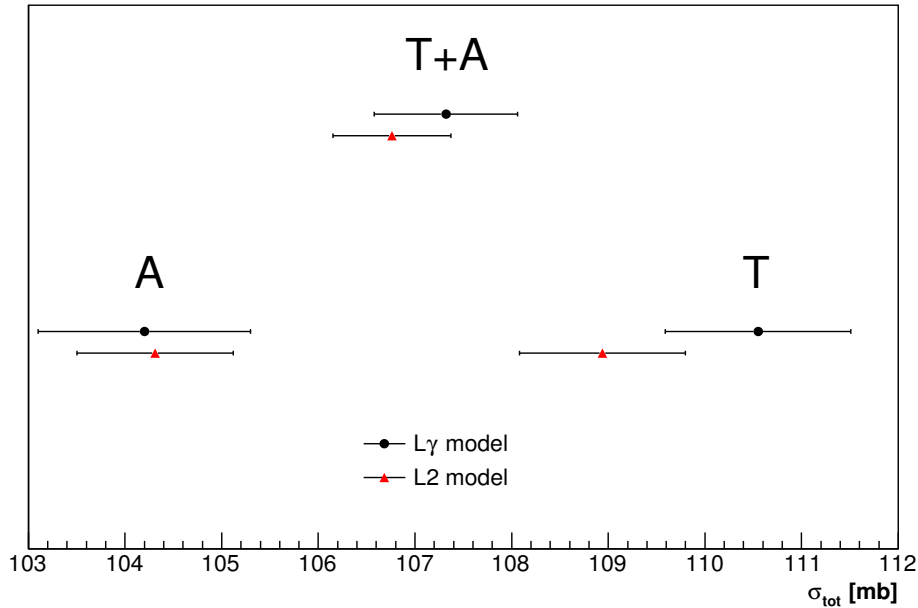


Figure 3: Predictions for σ_{tot} at 13 TeV within ensembles A, T+A and T and models L2 and L γ .

In our L γ model (with L2 as a particular case for $\gamma = 2$), the *analytic* connection between $\sigma_{tot}(s)$ and $\rho(s)$ is obtained through singly subtracted derivative dispersion relations, with the *effective subtraction constant* as a free fit parameter. Another analytic way to connect these two quantities is by means of asymptotic uniqueness (Phragmén-Lindelöf theorems) [39], Section 7.1. A detailed analysis, confronting these two analytic methods and the corresponding results for $\sigma_{tot}(s)$ and $\rho(s)$ is presented in [40].

Beyond providing useful parameters to quantify the different scenarios, the $\beta \ln^\gamma s$ leading term has also an interesting role in what concerns the rate of change of the total cross section. As a function of the variable $\ln s$, the Froissart, Lukaszuk, Martin bound for $\sigma_{tot}(\ln s)$ implies also in two bounds related to rates of change, namely the slope (S) and the curvature (C) for $s \rightarrow \infty$: linear ($2\beta \ln s$) and constant (2β) limits, respectively. On the other, the leading term predicts:

$$S = \beta\gamma \ln^{\gamma-1} s, \quad \text{and} \quad C = \beta\gamma(\gamma - 1) \ln^{\gamma-2} s,$$

thus allowing detailed investigations on the rate of change of the total cross section at high energies (not only $s \rightarrow \infty$). For example, at 8 TeV and with the L γ model, the fits with ensembles T and A predict: $S \sim 9.3 \pm 0.2$ mb (T) and $S \sim 7.9 \pm 0.3$ mb (A), indicating a faster rise of $\sigma_{tot}(s)$ from the TOTEM data than from the ATLAS data.

It is expected that further experimental analyses and the new data from LHC13 might clarify the different points and aspects raised in this work.

Acknowledgments

We are thankful to David D. Chinellato for useful discussions. Research supported by FAPESP, Contract 2013/27060-3 (P.V.R.G.S.).

Appendix A. Comments on the Dataset and Fit Procedure

Among the TOTEM data at 8 TeV, two points published in [27] and two points in [28] (see Table 1), correspond to different analyses based on the same dataset. Specifically, the two points from [27] are related to quadratic or cubic polynomials as parameterizations at the diffraction peak and those from [28] with central or peripheral phase formulations (Coulomb-nuclear interference region).

Therefore, in a certain sense, the two values in each pair of points might not be considered as independent data, as assumed in our analysis. In order to test the influence of this assumption (independent points), we have developed two re-analysis with the procedures that follow.

Firstly, we have estimated a mean value for each pair of points. Since the systematic uncertainties are the same (2.1 mb in [27] and 2.3 mb in [28]), in each case we have evaluated the arithmetic mean and the deviation from the mean, which was then added to the corresponding systematic uncertainties, resulting in two independent points: 101.7 ± 2.3 mb from [27] and 103.0 ± 2.4 mb from [28]. That seems a reasonable result since the deviation from the mean have a systematic character and adding with the real systematic uncertainty led to a larger uncertainty than that obtained by quadrature. By substituting these two independent estimations in place of the four points in ensembles T and T + A, the same fit procedure (explained in the text) led to the results presented in Table A.5.

Table A.5: Data reductions with the two TOTEM points from [27] and two from [28] (Table 1), substituted by their respective average estimations (see text). Fit results with models L2 and L γ to ensembles T and T+A. Parameters a_1, a_2, α, β in mb, K_{eff} in mbGeV² and b_1, b_2, γ dimensionless. Energy scale fixed, $s_0 = 4m_p^2 = 3.521$ GeV².

Ensemble:	TOTEM		TOTEM + ATLAS	
	L2	L γ	L2	L γ
a_1	32.11(61)	31.5(1.3)	32.21(69)	31.72(90)
b_1	0.389(18)	0.522(57)	0.414(16)	0.472(92)
a_2	16.99(71)	17.09(72)	17.02(72)	17.06(73)
b_2	0.545(13)	0.546(13)	0.545(13)	0.546(13)
α	29.51(47)	33.8(1.2)	30.28(33)	32.3(2.7)
β	0.2516(45)	0.109(32)	0.2423(29)	0.168(91)
γ	2 (fixed)	2.28(10)	2 (fixed)	2.12(18)
K_{eff}	53(18)	106(36)	64(18)	86(43)
ν	240	239	242	241
χ^2/ν	1.09	1.08	1.12	1.12
$P(\chi^2)$	0.151	0.196	0.089	0.089

In a second procedure, we have used the four points, but attributing a statistical weight equal to 1/2 to each one. The corresponding results are displayed in Table A.6.

Taking into account the uncertainties in free fit parameters and the number of degrees of freedom, comparison of Tables A.5 and A.6 shows that the two procedures led to practically

Table A.6: Data reductions attributing statistical weights equal to 1/2 to the four TOTEM points from [27] and [28] (Table 1). Fit results with models L2 and L γ to ensembles T and T+A. Parameters a_1, a_2, α, β in mb, K_{eff} in mbGeV² and b_1, b_2, γ dimensionless. Energy scale fixed, $s_0 = 4m_p^2 = 3.521$ GeV².

Ensemble:	TOTEM		TOTEM + ATLAS	
Model:	L2	L γ	L2	L γ
a_1	32.11(63)	31.5(1.3)	32.20(69)	31.70(64)
b_1	0.388(18)	0.522(69)	0.413(16)	0.473(57)
a_2	16.99(72)	17.09(73)	17.02(72)	17.06(72)
b_2	0.545(13)	0.546(13)	0.545(13)	0.546(13)
α	29.48(47)	33.9(1.4)	30.26(33)	32.4(1.6)
β	0.2520(44)	0.109(40)	0.2427(29)	0.166(55)
γ	2 (fixed)	2.28(13)	2 (fixed)	2.13(11)
K_{eff}	53(18)	106(41)	64(18)	86(29)
ν	242	241	244	243
χ^2/ν	1.09	1.07	1.12	1.12
$P(\chi^2)$	0.170	0.221	0.099	0.099

the same result. Moreover, comparison with the results displayed in Table 2 (four points treated as independents), shows that all values of the free parameters are in agreement within the uncertainties and the small differences in the goodness of fit are not relevant on statistical grounds.

We conclude that, in the present case, the three procedures led to numerical and statistical results that are equivalent.

References

- [1] M. Froissart, Phys. Rev. 123 (1961) 1053.
- [2] A. Martin, Phys. Rev. 129 (1963) 1432.
- [3] A. Martin, Nuovo Cimento A 42 (1966) 930.
- [4] L. Lukaszuk, A. Martin Nuovo Cimento A 52 (1967) 122.
- [5] U. Amaldi et al., Phys. Lett. B 66 (1977) 390.
- [6] C. Augier et al. (UA4/2 Collaboration), Phys. Lett. B 315 (1993) 503.
- [7] J.R. Cudell, K. Kang and S.K. Kim, Phys. Lett. B 395 (1997) 311.
- [8] J.R. Cudell *et al* (COMPETE Collaboration), Phys. Rev. D 65 (2002) 074024.
- [9] J.R. Cudell *et al* (COMPETE Collaboration), Phys. Rev. Lett. 89 (2002) 201801.
- [10] E.G.S. Luna and M.J. Menon, Phys. Lett. B 565 (2003) 123.

- [11] K. Igi and M. Ishida, Phys. Rev. D 66 (2002) 034023. Phys. Lett. B 622 (2005) 286.
- [12] M.M. Block and F. Halzen, Phys. Rev. D 70 (2004) 091901. Phys. Rev. D 72 (2005) 036006.
- [13] Olive K A *et al* (Particle Data Group), Chin. Phys. C 38 (2014) 090001
- [14] C. Patrignani *et al* (Particle Data Group), Chin. Phys. C 40 (2016) 100001.
- [15] M. Giordano, E. Meggiolaro, J. High Energy Phys. 1403 (2014) 002.
- [16] M. Giordano, E. Meggiolaro, Phys. Lett. B 744 (2015) 263.
- [17] D.A. Fagundes, M.J. Menon and P.V.R.G. Silva, Braz. J. Phys. 42 (2012) 452.
- [18] D.A. Fagundes, M.J. Menon and P.V.R.G. Silva, J. Phys. G: Nucl. Part. Phys. 40 (2013) 065005.
- [19] M.J. Menon, P.V.R.G. Silva, Int. J. Mod. Phys. A 28 (2013) 1350099.
- [20] M.J. Menon, P.V.R.G. Silva, J. Phys. G: Nucl. Part. Phys. 40 (2013) 125001; J. Phys. G: Nucl. Part. Phys. 41 (2014) 019501 [corrigendum].
- [21] Ya.I. Azimov, Phys. Rev. D 84 (2011) 056012.
- [22] G. Antchev *et al* (The TOTEM Collaboration), Europhys. Lett. 96 (2011) 21002.
- [23] G. Antchev *et al* (The TOTEM Collaboration), Europhys. Lett. 101 (2013) 21002.
- [24] G. Antchev *et al* (The TOTEM Collaboration) Europhys. Lett. 101 (2013) 21004.
- [25] G. Aad *et al* (The ATLAS Collaboration) Nucl. Phys. B 889 (2014) 486.
- [26] G. Antchev *et al* (The TOTEM Collaboration), Phys. Rev. Lett. 111 (2013) 012001.
- [27] G. Antchev *et al* (The TOTEM Collaboration), Nucl. Phys. B 899 (2015) 527.
- [28] G. Antchev *et al* (The TOTEM Collaboration), Eur. Phys. J. C 76 (2016) 661. arXiv:1610.00603 [nucl-ex].
- [29] M. Aaboud *et al* (The ATLAS Collaboration), Phys. Lett. B 761 (2016) 158.
- [30] K. Kang and B. Nicolescu, Phys. Rev. D 11 (1975) 2461.
- [31] R.F. Ávila and M.J. Menon, Nucl. Phys. A 744 (2004) 249.
- [32] Reference [14], <http://pdg.lbl.gov/2016/hadronic-xsections/hadron.html>.
- [33] G. Aielli *et al.* (ARGO-YBJ Collaboration), Phys. Rev. D 80 (2009) 092004.
- [34] P. Abreu *et al.* (The Pierre Auger Collaboration), Phys. Rev. Lett. 109 (2012) 062002.

- [35] U. Abbasi et al. (Telescope Array Collaboration) Phys. Rev. D 92 (2015) 032007; Erratum Phys. Rev. D 92 (2015) 079901.
- [36] ROOT Framework, <http://root.cern.ch/drupal/>;
<http://root.cern.ch/root/html/TMinuit.html>.
- [37] F. James, MINUIT Function Minimization and Error Analysis, Reference Manual, Version 94.1, CERN Program Library Long Writeup D506 (CERN, Geneva, Switzerland, 1998).
- [38] P.R. Bevington and D.K. Robinson, Data Reduction and Error Analysis for the Physical Sciences, McGraw-Hill, Boston, Massachusetts, 1992.
- [39] Eden R J, High Energy Collisions of Elementary Particles, Cambridge University Press, Cambridge, 1967, Chapter 7.
- [40] D.A. Fagundes, M.J. Menon and P.V.R.G. Silva, “Leading components in forward elastic hadron scattering: Derivative dispersion relations and asymptotic uniqueness”, arXiv:1705.01504 [hep-ph].